Journal of Membrane Science 516 (2016) 64–73

Contents lists available at ScienceDirect

Journal of Membrane Science

journal homepage: www.elsevier.com/locate/memsci

Investigating the significance of coagulation kinetics on maintaining membrane permeability in an MBR following reactive coagulant dosing

O. Autin [a], F. Hai [b], S. Judd [a], E.J. McAdam [a,*]

[a] Cranfield Water Science Institute, Vincent Building, Cranfield University, Bedfordshire, MK43 0AL, UK
[b] Strategic Water Infrastructure Laboratory, School of Civil, Mining and Environmental Engineering, University of Wollongong, Wollongong, NSW 2522, Australia

ARTICLE INFO

Article history:
Received 17 March 2016
Received in revised form
3 June 2016
Accepted 4 June 2016
Available online 11 June 2016

Keywords:
Membrane performance enhancer
Membrane bioreactor
Direct visual observation

ABSTRACT

In this study, the impact of kinetically controlled floc growth on sustaining membrane permeability following reactive coagulant dosing was determined using a model particle system. Floc formation was indicated to comprise of two stages following coagulant addition: (i) an initial destabilisation phase which encouraged complexation of protein and polysaccharide; and (ii) entrapment of the coarse model particles (3 μm Firefli™ microspheres) in the polymeric complex during the floc growth phase. Floc growth was characterised by an expected time lag as with conventional flocculation systems and biopolymer aggregation was kinetically favoured. When coagulant was dosed during the filtration cycle, the intermediate biopolymer aggregates (comprised of protein and polysaccharide) were preferentially transported toward the membrane increasing fouling. However, when coagulant was dosed at the onset of filtration, membrane fouling was constrained. It is asserted that by dosing at the onset of filtration: (i) early development of biopolymer aggregation is initiated which inhibits transport of the individual biopolymers to the membrane; and (ii) by dosing coagulant in the absence of a developed polarised layer, formation of biopolymer complexes local to the membrane is obviated. However, when dosing coagulant at the onset of filtration, only limited floc growth occurred which can be explained by the low applied wall shear rate and the absence of a 'polarised' region which ostensibly promoted floc growth when coagulant was dosed mid-filtration. Based on results from the model particle system studied, it is proposed that reactive coagulant dosing is best undertaken when: (i) filtration is stopped; (ii) modest shear is applied within the bioreactor to promote coagulant dispersion; and (iii) sufficient contact time is allowed to promote floc growth before commencement of filtration.

1. Introduction

Membrane bioreactors (MBRs) have become a standard technology for wastewater treatment. However, understanding how to ensure sustained membrane permeability remains a key operational consideration [4,15]. Several approaches have been introduced in order to reduce fouling including intermittent suction [16], backflushing [17], module design improvement [21] or the optimisation of aeration such as with the LEAPmbr aeration technology which has enabled dramatic reductions in operational energy cost to be realised [8]. Nevertheless membrane fouling remains important, particularly understanding how to respond to system perturbation, and as such it is suggested that MBR cost could be further reduced by better control of membrane fouling [20].

Membrane fouling is a consequence of the interaction between the membrane and a complex mixture comprising colloids, bacterial flocs and dissolved macromolecules [21]. It has been widely reported that soluble microbial products (SMP) which comprise mainly of proteins and polysaccharides are primarily responsible for the clogging and blocking of membrane pores [22,23]. As these compounds are generally colloidal in nature, their transport is primarily controlled by Brownian motion and as such the shear forces applied either through pumping (in side stream) or aeration (in immersed) are insufficient to provide back-transport toward the bulk which results in preferential colloidal deposition at the membrane [29]. Deposition of these high molecular weight compounds result in formation of a highly hydrated gel matrix into which microorganisms are embedded, resulting in a significant resistance to permeate flow during membrane operation [25].

To ameliorate the potential impact of SMP on membrane fouling, several authors have introduced the use of coagulants [4,5,20,24] which enable the assimilation of SMP compounds into aggregates (or flocs), that are then more strongly influenced by

* Corresponding author.
E-mail address: e.mcadam@cranfield.ac.uk (E.J. McAdam).

http://dx.doi.org/10.1016/j.memsci.2016.06.008

inertial lift and shear induced diffusion, thereby promoting back-transport away from the membrane surface into the bulk [20,24]. Numerous chemical compounds have been trialled including metal salts, biopolymers, starch [4,5] and organic polymers and have been considered particularly pertinent for reactive dosing of the coagulant to limit the impact of sudden SMP release in response to process perturbation, such as saline shock [6,9,10]. Woznaik [24] described the use of MPE50 which is a modified biopolymer with a net cationic charge that has been demonstrated to effectively reduce membrane fouling both at laboratory and full scale [4,5,24]. Hwang et al. [14] suggested that the cationic structure of MPE50 enabled the neutralisation of the negatively charged colloidal biopolymers, thereby encouraging floc growth, which can be considered analogous to conventional coagulation-flocculation. However, in conventional application, coagulation and flocculation processes are generally configured in series. In the coagulation step, coagulant is added within a high shear zone with an average velocity gradient (G) exceeding 1500 s^{-1} to ensure the coagulant is distributed homogeneously in order to achieve particle destabilisation and charge neutralisation. Flocculation then proceeds in a secondary shear zone with a gentler average velocity gradient of around 100–200 s^{-1} to encourage successful collision of destabilised particles and is provided with a retention time of up to 60 min to ensure subsequent floc growth is complete [3].

For comparison, there is no high shear zone specified within present MBR design to incorporate coagulant dosing. Furthermore, the average velocity gradient imposed by coarse bubble aeration in MBR is around 150–200 s^{-1} [11–13]. Consequently, without a clearly delineated high shear zone to provide homogeneous distribution of the coagulant, and with gas mixing in MBR providing a velocity gradient which is equivalent to flocculation, it is suggested that coagulation-flocculation will be rate limited within MBR which will cause a delay in the time from which coagulant is reactively dosed to when colloids destabilise and form aggregates. As flocculators are generally designed with residence times of up to 60 min to enable sufficient time for aggregate growth, it is posited that with direct dosing of MPE50 into the MBR, the time at which coagulant is added during the filtration cycle could therefore be of significance to sustaining membrane permeability during filtration. The aim of this study is therefore to establish the significance of coagulation-flocculation kinetics on membrane permeability following the reactive dosing of coagulant. The widely used commercially available cationic polymer MPE50 was employed as the coagulant and a model particle suspension was employed to provide a controlled testing environment, comprising of the biopolymers bovine serum albumin (BSA) and sodium alginate (Na-alginate), as surrogates for protein and polysaccharide, and 3 μm Firefli™ microspheres were included to provide a bimodal size distribution characteristic of an MBR sludge .

2. Material and methods

2.1. Cross-flow cell linked with direct visual observation

The crossflow cell was constructed of Perspex and comprised a flow channel with a width of 0.012 m, length 0.21 m and height 0.006 m. A viewing window was engineered within a recess of the upper cell wall (Fig. 1). The opening was lined with an o-ring to provide a watertight seal to a coverslip ($n=1.5$, or 0.17 mm thick) which was held in place by an annular clamp. The microscope (Leica DM5500B Microsystems, Milton Keynes, UK) was fitted with a HC PL FL 10X/0.30 lens which provided a wide range of free working distance (around 11 mm) which is sufficient to incorporate the depth of field below the viewing window to the membrane surface. A Polyvinylidene fluoride (PVDF) hollow fibre membrane with a nominal pore size of 0.04 μm (Zeeweed, GE Power and Water, Ontario, USA) was used in this study and had an outside diameter of 0.0019 m, yielding an active membrane surface area of 0.00125 m^2. The depth from the outer diameter of the hollow fibre membrane to the underside of the viewing window was around 2.5 mm which was sufficient to allow active fluid transport around the fibre.

The microscope used for direct observation was fitted with a high speed, high-sensitivity digital camera (DFC365 FX, Leica Microsystems, Milton Keynes, UK) for image and video recording. Analysis of cake height using static images was undertaken using Leica Application Suite software. To quantify particle back transport velocity from video footage, VideoStudio software was used (Ulead, Malavida). To enhance particle tracking, a fluorescence

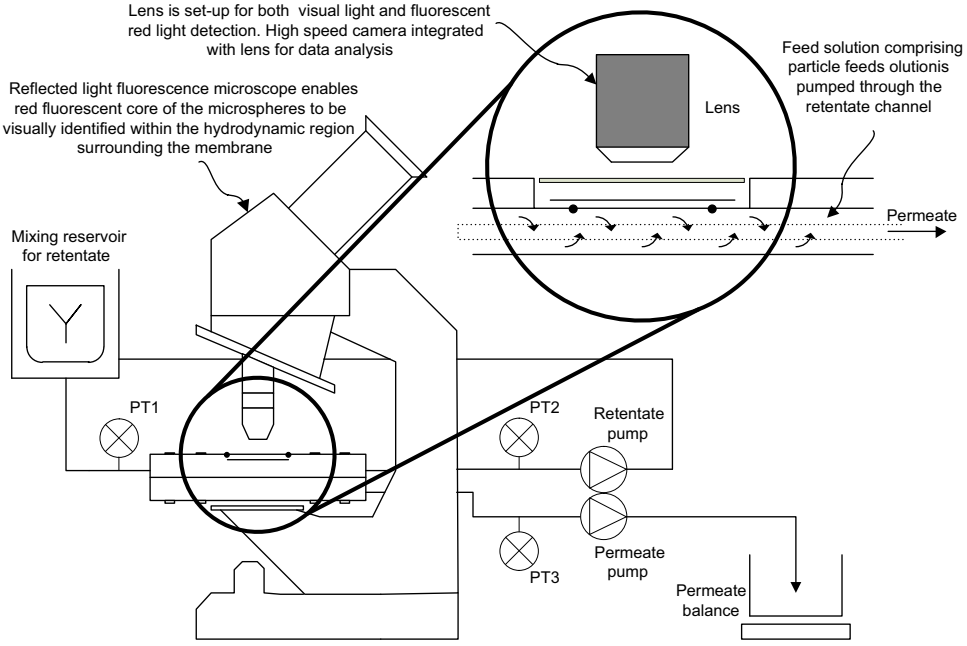

Fig. 1. Experimental set-up comprising direct visual observation cell equipped with reflected light fluorescence microscope.

enabled microscope was used in conjunction with Firefli™ fluorescent red 3 μm polystyrene microspheres which exhibited excitation/ emission at 542/612 nm. At the specified V_L (0.011 m s^{-1}) and particle concentration (25 mg l^{-1}) visual determination of individual particles with diameters exceeding 0.5 μm can be achieved using this reflected light fluorescence direct visual observation method [19].

Feed solution was recirculated at a velocity (V_L) of 0.011 m s^{-1} through the retentate channel (520S, Watson Marlow, Falmouth, UK). This represents a Reynold's number (Re) of 88 which is indicative of laminar flow. Since the relative flux is low with respect to V_L, and making the assumption of a rectangular channel, shear rate (γ_0) was fixed to 11 s^{-1}. Both permeate and retentate were fed back to the feed reservoir, which was only slowly mixed to avoid sedimentation. Each permeability assessment was undertaken over 120 min at a fixed flux of 100 l m^{-2} h^{-1}. To determine transmembrane pressure (TMP), pressure transducers (PT) were sited on the permeate line (−0.5 to +0.5 bar(g)), upstream and downstream of the retentate channel (0–1 bar(g)). Each PT had a reported sensitivity of less than 0.25% of range. The analogue signal arising from each PT was collected with an ADC-24 data logger and analysed with the Picolog data acquisition software (Pico technology, St Neots, UK). Fluid temperature was controlled at 20 °C. Permeate was collected on a balance (Symmetry PR-precision toploading balance, Cole-Parmer, London, UK) and the mass recorded directly onto a PC. Residual resistance from caking, pore plugging and irreversible adsorption (R_{res}) was calculated from [18,29]:

$$R_m = \frac{\Delta TMP}{\mu J_W} \quad (1)$$

$$R_{res} = \frac{\Delta TMP}{\mu J_{ps}} - R_m \quad (2)$$

where R_m is the membrane resistance determined during the filtration of deionised water at flux, J_w (100 l m^{-2} h^{-1}), and J_{ps} is the flux used for filtration of the particle solution. Reproducibility of TMP data produced from the experimental set-up was assessed using the full particle matrix (sodium alginate, bovine serum albumin and 3 μm microspheres) and an average error of 16% recorded between replicates (Fig. 2).

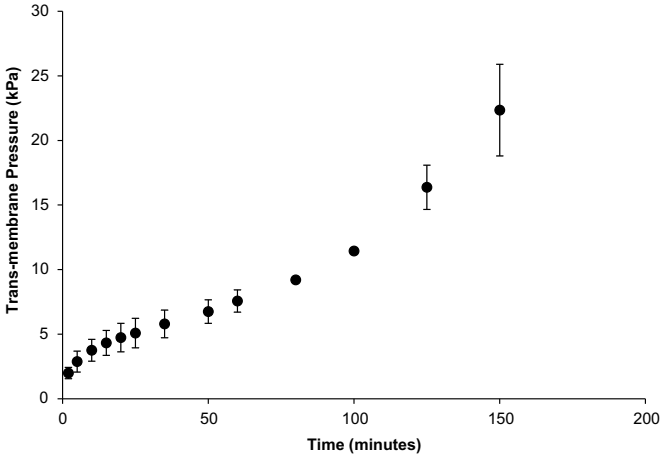

Fig. 2. TMP profile during filtration of 50 mgBSA l^{-1}, 50 mgNa-Alg l^{-1} and 25 mg l^{-1} of 3 μm particles for several experiments (average error from mean, 16%). Cross-flow velocity 11 mm s^{-1} (wall shear rate 11 s^{-1}); flux 100 l m^{-2} h^{-1}.

2.2. Chemicals and analytical methods used

Bovine serum albumin (BSA, 200 mg mL^{-1}) and sodium alginate (Na-alg,) were used as model biopolymers (Sigma-Aldrich, Poole, UK). Fluorescent enabled 3 μm latex microspheres were used to provide a bi-modal particle size distribution, providing a strictly controlled particle diameter (uniformity < 5%) and shape that are also easily traceable within a complex matrix owing to their fluorescent core (Fisher Scientific, Loughborough, UK). Model solutions were prepared using initial concentrations of fluorescent microspheres, sodium alginate and BSA of 25 mg l^{-1}, 50 mg l^{-1} and 50 mg l^{-1} respectively, diluted in ultrapure water (Purelab Option – S7/15, 18.2 MΩ cm^{-1} and TOC < 3 ppb) to which 20 mM sodium chloride (NaCl) and 1 mM sodium hydrogen carbonate ($NaHCO_3$) were added to increase ionic strength and buffering capacity of the water (Fisher Scientific, Loughborough, UK). After each experiment, the membrane was rinsed with ultrapure water for 15 min, followed by a backwash operation at 40 l m^{-2} h^{-1} for 15 min and then chemically cleaned overnight with 500 mg L^{-1} of sodium hypochlorite solution (Sigma-Aldrich, Poole,). The cationic polymer MPE50 was selected for use in this study, the efficiency of which has been previously demonstrated in MBR matrices following screening a broad range of potential additives [4]. As such, a comparison with other potential polymers was not made. The chemical MPE50 was kindly supplied by Nalco (Leiden, The Netherlands).

Zeta potential was determined using laser Doppler electrophoresis (Malvern Zetasizer 2000, Malvern Instruments Ltd., Malvern, UK). Particle size was measured using laser diffraction (Malvern Mastersizer 2000, Malvern Instruments, UK). Protein and polysaccharide concentrations were quantified using the modified Lowry method [27] and phenol-sulfuric acid method [28] respectively. Kinetic experiments were undertaken on a jar tester to determine the rate of aggregation initiated following inclusion of MPE50. Jar tester samples were prepared in 1 L samples and were subject to a stirring at 50 rpm, equivalent to a mean velocity gradient (G) of 44 s^{-1}.

3. Results

3.1. Determination of an appropriate MPE50 dose for the particle matrix

The efficacy of MPE50 for removing biopolymers from bulk solution into aggregates was assessed within water comprising a particle complex of 50 mg l^{-1} of the protein Bovine Serum Albumin (BSA), 50 mg l^{-1} of the polysaccharide sodium alginate (Na-Alg) and 25 mg l^{-1} of 3 μm particles (Fig. 3). An increase in the removal of BSA from 3% to 18% was demonstrated following an increase in MPE50 dose from 1 to 200 mg l^{-1} (Fig. 3(a)). However, a plateau was reached once the MPE50 dose had increased above 200 mg l^{-1}, which suggested that further increase in protein removal efficiency was not attainable. Sodium alginate removal efficiency increased from 5% to 65% once MPE50 dose increased from 100 mg l^{-1} to 200 mg l^{-1} and then markedly declined to 23% upon increasing the MPE50 dose to 500 mg l^{-1} (Fig. 3(b)). This is analogous to behaviour observed by [4] when dosing MPE50 within a similar concentration range to promote coagulation of protein and polysaccharides derived from soluble microbial products (SMP) produced from an MBR.

3.2. Aggregation and floc growth for the particle matrix following MPE50 dosing

Zeta potential of the individual biolpolymers and of the

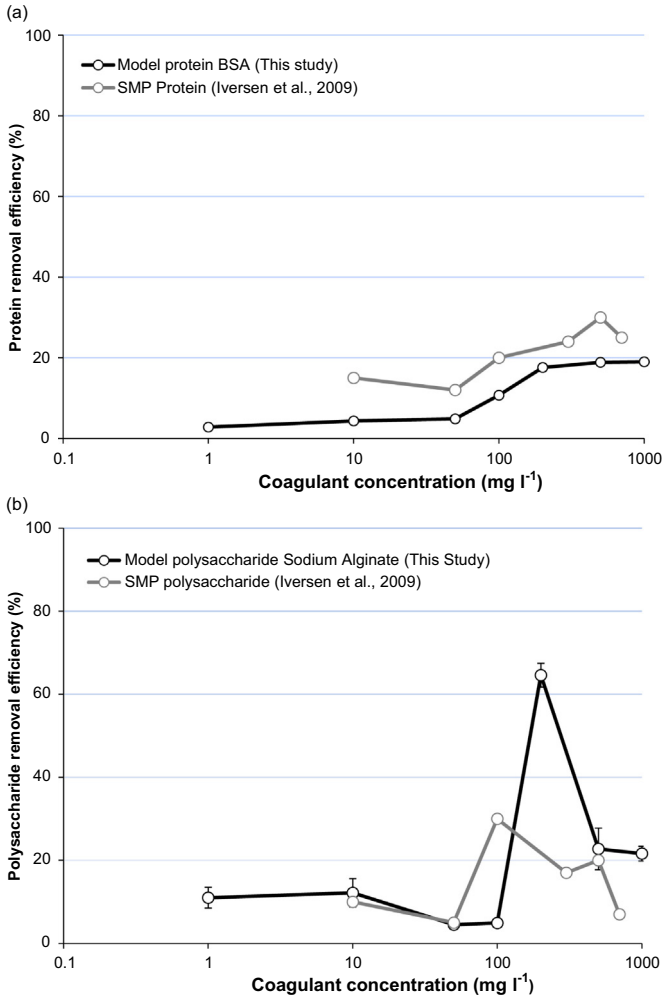

Fig. 3. Characterisation of coagulant dose in the model system comprising 50 mgBSA l^{-1}, 50 mgNa-Alg l^{-1} and 25 mg l^{-1} of 3 μm particles. Reference data for MPE50 dosing in MBR sludge extrapolated from [4].

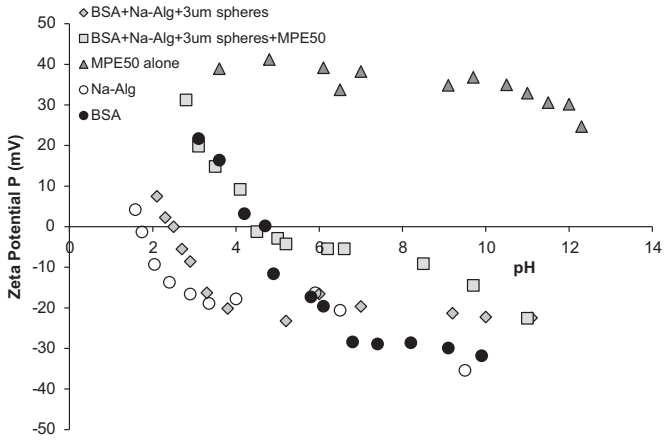

Fig. 4. Zeta potential of single and complex systems.

combined particle matrix was determined (Fig. 4). Isoelectric points (IEP) of pH 1.7 and pH 4.7 were determined for Na-Alg and BSA respectively which are coincident with the literature [7]. The zeta potential of MPE50 varied between 38.9 mV and 24.7 mV across the pH range evaluated (pH 3.6–12.3). When each of the particle types were combined within one solution (BSA, Na-alg and 3 μm particles), the zeta potential curve was between those

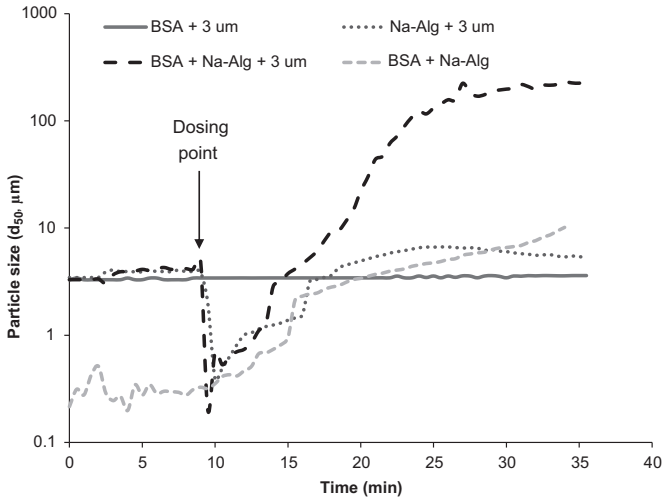

Fig. 5. Particle size analysis undertaken for systems of increasing particle complexity (Malvern Mastersizer, 2000, Malvern Instruments). A 200 mg l^{-1} MPE50 dose added after around 10 min.

recorded for BSA and Na-Alg and subsequently shifted to the right following a 200 mg l^{-1} addition of MPE50.

The effect of both MPE50 and particle type on final aggregate size was determined (Fig. 5). MPE50 was dosed 10 min after the trial commenced. When either BSA or Na-alg was combined with 3 μm spheres, the impact of MPE50 addition on floc growth was negligible. When MPE50 was dosed into a mixture of Na-alg and BSA, particle size increased from less than 1 μm to over 9 μm. A notable increase in particle size was observed through addition of 3 μm spheres to the Na-alg/BSA mixture, reaching a maximum d_{50} of 230 μm around 20 min after MPE50 addition.

3.3. Establishing uptake rate of biopolymers into the floc following MPE50 dosing

The kinetics of aggregation was studied in batch using the complete particle matrix comprising 50 mgBSA l^{-1}, 50 mgNa-alg l^{-1} and 25 mg l^{-1} of 3 μm particles. Following application of a 200 mg l^{-1} dose of MPE50 to the particle matrix, water samples were subject to filtration through 0.22 μm, 0.45 μm, 2.7 μm and 8 μm membranes. The remaining sodium alginate and BSA concentrations resident in each permeate fraction then provided indication of the minimum size of aggregate that the biopolymers had assimilated into following dosing (Figs. 6 and 7).

An initial assessment of the impact of the various fractions of the particle matrix was undertaken using (a) BSA/ sodium-alginate, (b) sodium alginate/3 μm particles, and finally (c) the complete particle matrix comprising BSA/sodium-alginate/3 μm particles (Fig. 6). During batch testing, the highest uptake of sodium alginate into larger aggregates following MPE50 addition was determined for the BSA/sodium alginate and BSA/sodium alginate/ 3 μm particle mixtures (around 30 mg l^{-1} consumed). However, the rate coefficient (k) which described the rate of uptake of sodium-alginate into aggregates greater than 8 μm was markedly higher for the BSA/sodium alginate mixture (k 0.11 min^{-1}) than for the sodium alginate/3 μm and BSA/sodium alginate/3 μm mixtures which were 0.01 min^{-1} and 0.05 min^{-1} respectively (Fig. 7(a)). Analysis of the rate of uptake of both sodium-alginate and BSA within the complete particle mixture (sodium-alginate/ BSA/3 μm spheres) demonstrated uptake into smaller aggregates was considerably higher than larger aggregates and furthermore that protein followed a similar trend to sodium alginate but the established rate of uptake into aggregates was considerably faster (Fig. 7(b)).

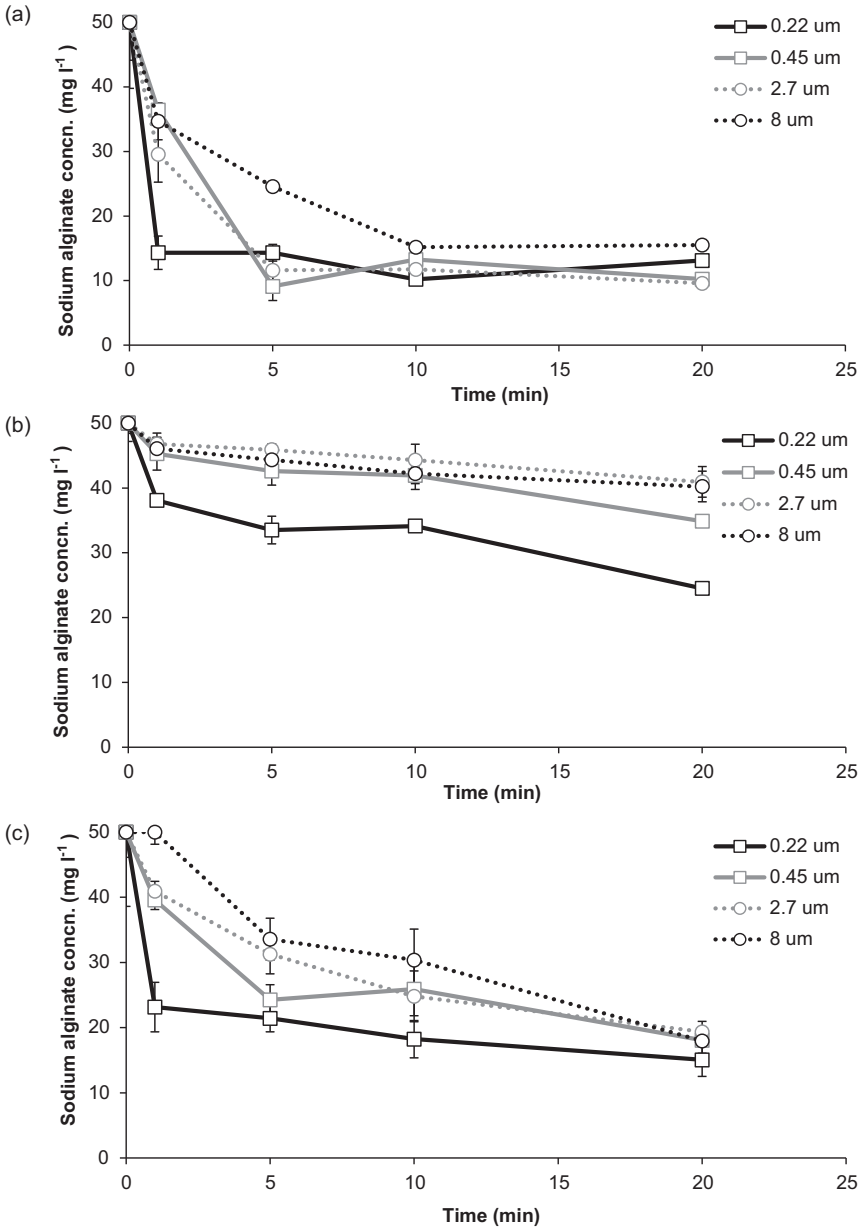

Fig. 6. Determination of the kinetics of aggregation amongst the individual particulate constituents: (a) BSA (50 mg l^{-1}), Sodium alginate (50 mg l^{-1}), MPE50 (200 mg l^{-1}); (b) Sodium alginate (50 mg l^{-1}), 3 μm particles (25 mg l^{-1}), MPE50 (200 mg l^{-1}); (c) BSA (50 mg l^{-1}), Sodium alginate (50 mg l^{-1}), 3 μm particles (25 mg l^{-1}), MPE50 (200 mg l^{-1}).

3.4. Impact of reactive MPE50 dosing on membrane fouling

The control test used a complex comprising of BSA, Na-alg and 3 μm Firefli™ microspheres but without the addition of MPE50 (Fig. 8). The TMP profile comprised of a classical two stage shape where an initial filtration stage characterised by a dP/dt_{phase1} 0.08 kPa min^{-1} was followed by a sharp rise in TMP of dP/dt_{phase2} 0.87 kPa min^{-1} at around 55 min leading to a final residual resistance (R_{res}) of 56×10^{10} m^{-1} recorded after 120 min of filtration. Dosing of MPE50 was undertaken at 0 and then 30 min after filtration had commenced to ascertain the importance of dosing time for reactive control of membrane fouling (Fig. 8). For the first 30 min of filtration, the growth in cake resistance was ostensibly similar to that without MPE50 addition. However, following further filtration, cake resistance declined and was coincident with a reduction in cake height from a maximum of 10 μm, measured after 15 min of filtration, to below 3 μm when measured after 120 min of filtration. When MPE50 dosing was applied 30 min after filtration, a marked increase in residual resistance was immediately observed (Fig. 8).

Before dosing of MPE50, direct observation evidenced axial migration of 3 μm Firefli™ particles in the bulk flow (circled in red) above a small static cake (< 5 μm) which had formed at the membrane surface (Fig. 9(a)). Within one minute of dosing MPE50 at 30 min, a fluidised cake of around 25 μm in depth was noted to have formed above the static cake (Fig. 9(b)). Several individual 3 μm Firefli™ particles were observed within this fluidised layer. However, due to the low number density of 3 μm particles present within this fluidised polarised region above the stagnant cake, it was postulated that this was predominantly comprised of the biopolymers BSA and sodium alginate. Direct observation of the membrane wall 15 min after dosing evidenced that the fluidised layer had dissipated and growth of large aggregates had initiated which were visibly observed to undergo axial migration in the

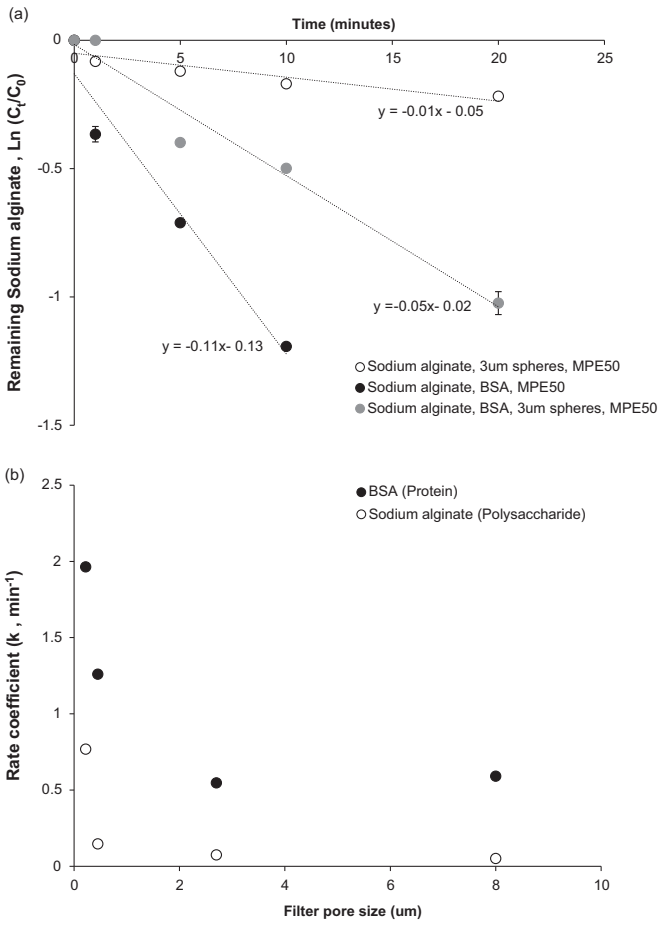

Fig. 7. (a) Derivation of the rate coefficient from the aggregation experiments undertaken with different particle compositions in the presence of MPE50. Analysis of the <8 μm fraction shown; (b) The final rate coefficient determined for the full particle matrix (BSA, Sodium alginate, 3 μm spheres, MPE50) within each filtered fraction.

bulk flow away from the membrane wall, as well as floc rolling along the membrane surface in the direction of flow (Fig. 9(c)). The formation of the fluidised region immediately after dosing MPE50 at 30 min coincided with a rapid increase in R_{res} of over 800% to 16.1×10^{10} m^{-1}. Residual resistance did not markedly increase following continued filtration and the final R_{res} measured at 120 min was lower than in the absence of coagulant (Fig. 8). A fluidised region was not observed when MPE50 was dosed at the commencement of filtration (0 min), although a final R_{res} of 1.2×10^{10} m^{-1} was recorded which is an order of magnitude below the cake resistance recorded following MPE50 dosing at 30 min after filtration had commenced (R_{cake} 19×10^{10} m^{-1}).

Fluorescence microscopy was used to evidence the presence of 3 μm Firefli™ particles within the aggregates formed following MPE 50 dosing (Fig. 10). Volume and concentration constrained the capability to use standard methods (e.g. laser diffraction) for particle size distributions. However, the comparative images qualitatively evidence the formation of considerably larger aggregates of around 80 μm following MPE50 dosing at 30 min. Interestingly, whilst the addition of MPE50 at 0 min of filtration resulted in the lowest final cake resistance, it is also the condition in which the aggregates were the smallest, stabilising at around 10 μm in size after only 5 min following MPE50 dosing. Particle velocity of the 3 μm Firefli™ particles in the polarised region of the membrane was also ascertained (Fig. 11). At the onset of filtration, particle velocity was approximately 800 μm s^{-1} at a distance of 60 μm from the membrane surface. This value is much lower than the superficial liquid velocity of 11 mm s^{-1} (V_{SL} 11,000 μm s^{-1}) indicating the heterogeneous distribution of fluid velocity within the channel as previously demonstrated by [26]. When MPE50 dosing was not applied (Fig. 11(a)), the apparent particle velocity was greatly reduced. To illustrate, after only 60 min of filtration, apparent particle velocity at 60 μm from the membrane surface was less than 200 μm s^{-1} and the 3 μm Firefli™ particles were ostensibly increasingly captured by the development of a viscous gel. In contrast, when using MPE50, the apparent particle velocity was maintained reasonably constant for the duration of the filtration cycle, measuring over 400 μm s^{-1} after 120 min of filtration (Fig. 11(b) and (c)).

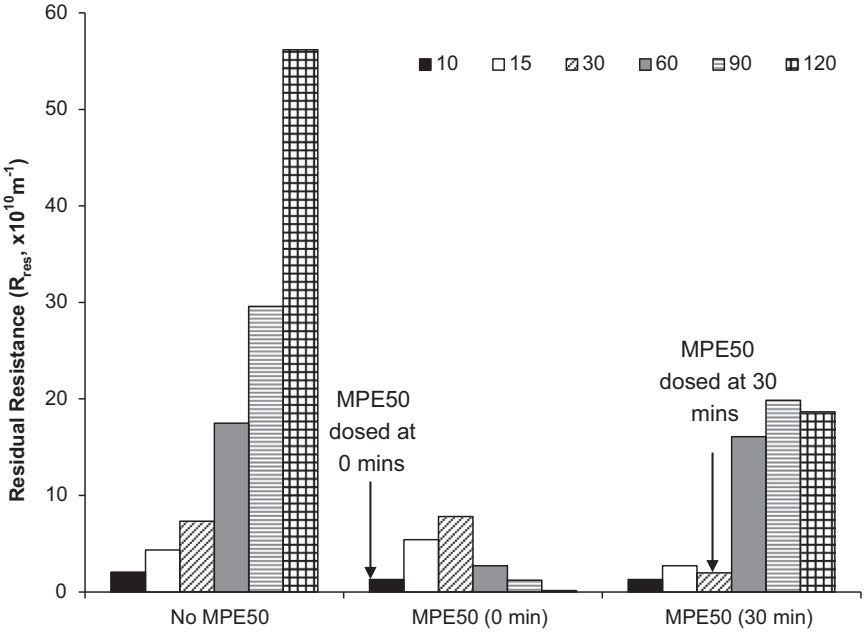

Fig. 8. Residual resistance determined during the course of filtration for a particle complex comprising 50 mg l^{-1} BSA, 50 mg l^{-1} Sodium alginate and 25 mg l^{-1} 3 μm spheres. For tests conducted with MPE50 (dosing times of 0 mins and 30 mins after filtration is initiated), a 200 mg l^{-1} dose was applied. Cross-flow velocity, 11 mm s^{-1}; flux 100 l m^{-2} h^{-1}.

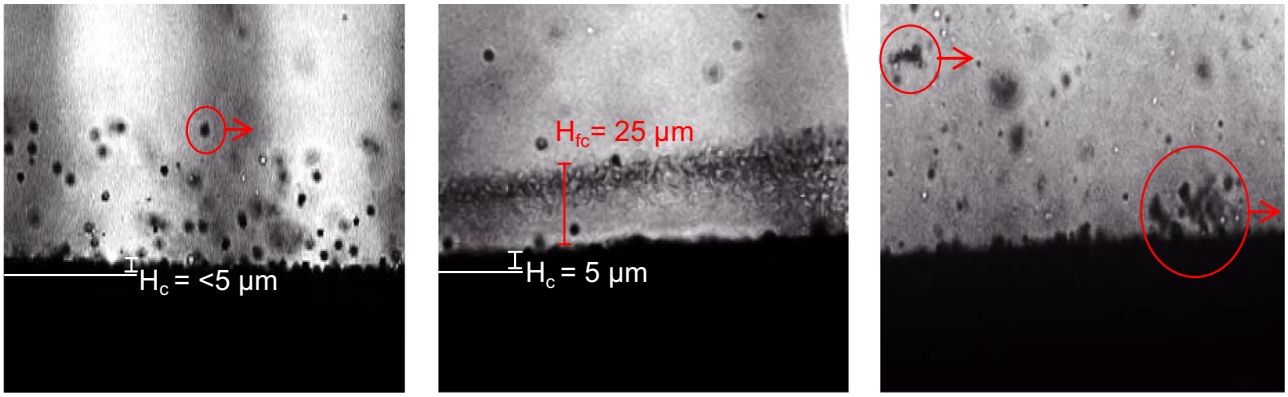

Fig. 9. Direct observation of fouling before and after the addition of MPE50 at the 30 min dosing point: a) 2 min before MPE50 addition; b) 1 min after MPE50 addition); and, C) 15 min after MPE50 addition.

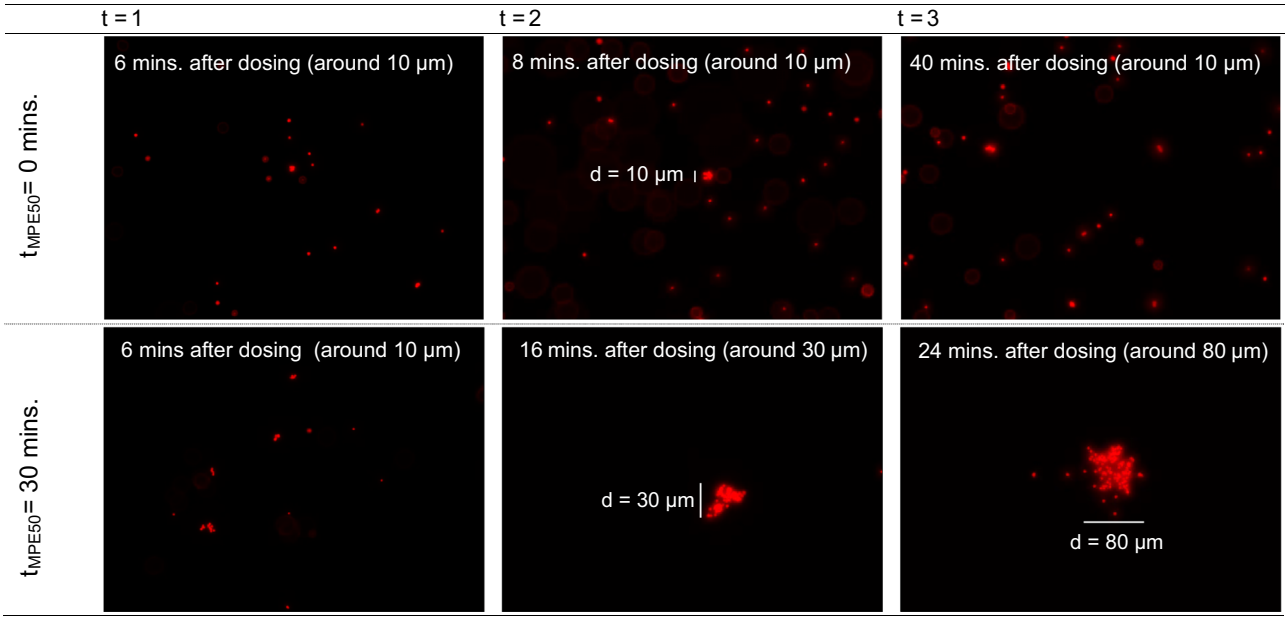

Fig. 10. Aggregates visualised in the retentate channel following injection of MPE50.

4. Discussion

In this study, the significance of coagulation kinetics on the stabilisation of membrane permeability following the reactive dosing of coagulant has been investigated within a model particle system comprising of a bimodal particle size distribution. An optimum MPE50 dose of 200 mg l^{-1} was identified by a 'peak' in polysaccharide removal efficiency and is analogous to previous observation of dosing MPE50 into real SMP where introducing an excess of chemical resulted in deflocculation [4,5]. Koseoglu et al. [5] explained this phenomenon by the adsorption of excess cationic polymer which then reversed the surface charge to net positive thereby promoting deflocculation via electrostatic repulsion. Importantly, the MPE50 dose identified in this study is within the range typically used in industry and resulted in elimination of between 10 and 30 mg l^{-1} of biopolymer which is coincident with the literature (Fig. 3). However, substantive flocculation was noted only to occur within bimodal particle systems when both protein and polysaccharide were present together (3 µm: Na-alg:BSA, d_{50} over 200 µm, Fig. 5). Hwang et al. [14] determined a d_{50} floc size of 179 µm when maintenance dosing MPE50 into the activated sludge of an MBR which compared to a d_{50} of only 101 µm without dosing. In this study, it is asserted that the first stage of flocculation was the initial formation of aggregates comprised of BSA and Na-alginate. This is analogous to behaviour observed by [7] in which formation of BSA: Na-alg soluble complexes was promoted by lowering zeta potential sufficient to permit the positively charged micro-regions on the protein to bind onto the negatively charged carboxyl groups on the alginate. Measurement of the aggregation kinetics confirmed that the assimilation of Na-alginate into aggregates is augmented when in the presence of BSA (Fig. 7 (a)). Wilen et al. [30] positively correlated protein contained within the extracellular polymeric substances (EPS) to flocculating ability of activated sludge. This can be ascribed to the numerous multifunctional charged groups resident within the polypeptide structure of proteins that can promote aggregation [7] and was evidenced in this study by the high rate coefficient determined for the uptake of protein within the flocs formed when present in the complete particle mixture (Fig. 7(b)). It is therefore suggested that flocculation within this model particle system proceeds by the initial aggregation of BSA: Na-alginate into a polymer network, which then traps and embeds the 3 µm particles within their structure.

During filtration experiments, this initial phase of aggregation between BSA and Na-alginate was identified by the formation of a large fluidised cake (25 µm, Fig. 9(b)) which formed in the region local to the membrane surface after MPE50 was added 30 min into filtration (Fig. 9). Jiang et al. [1] undertook modelling of the

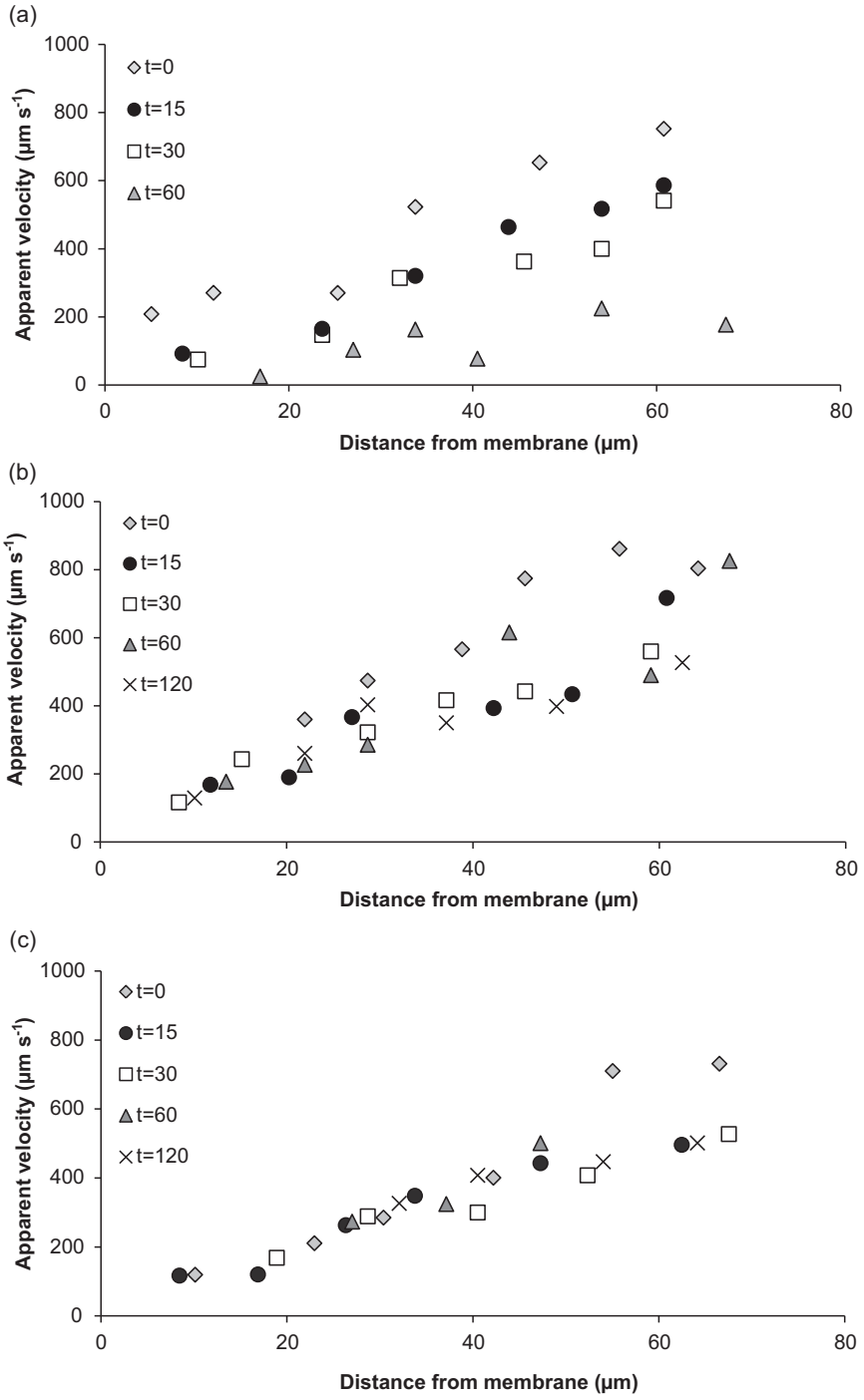

Fig. 11. Particle transport velocity in fluidised region at differing time intervals during filtration. Experimental conditions as follows: (a) without addition of MPE50; (b) addition of MPE50 at commencement of filtration (0 min); and, (c) addition of MPE50 following a period of filtration.

backtransport velocity for a particle size range symptomatic of the bimodal distribution ordinarily noted in MBR studies and showed that submicron particles (such as biopolymers) had a high probability for deposition at the membrane surface as the convective forces employed during filtration often exceeded the shear forces applied by CFV, even within side-stream systems where CFV exceeding 0.5 m s^{-1} are often employed. In this study, it is asserted that the fluidised cake was formed following diffusion of MPE50 into a concentrated region of BSA and Na-alginate which had polarised local to the membrane surface as the shear conditions promoted by the CFV employed were insufficient to provide back transport for this particle size group (γ_0, 11 s^{-1}). A considerable rise in TMP was coincident with the development of the fluidised cake (Fig. 8). Thus whilst the addition of MPE50 reduced zeta potential, it is postulated that fouling was dominated by deposition within the polarised layer rather than specifically through promotion of particle-membrane interaction [7,31]. Neemann et al. [7] identified that it was at the initiation of the non-covalent protein-polysaccharide network where the highest fouling rate was determined. It is therefore suggested that this initial stage of protein-polysaccharide aggregation caused the formation of small particles (of around 10 μm or less, Fig. 5) which preferentially migrated toward the membrane forming a highly resistive cake layer. Around fifteen minutes after MPE50 was added, the fluidised

cake had dissipated and large aggregates were seen to have developed (Fig. 9(c)) which were evidenced to comprise of 3 μm Firefli™ microspheres (Fig. 10). The formed aggregates were seen to be transported within the bulk flow in addition to undergoing migration through 'floc rolling' along the membrane wall. This migratory behaviour can be accounted for by the increased particle size which enhances back transport. To illustrate, using the shear induced diffusivity (SID) model set out in [2] (Eq. (3)), particles with diameters exceeding 80 μm could be subject to SID forces that would balance the convective force of permeation and hence favour particle migration away from the membrane surface:

$$J = 0.0595\gamma_0\left(\frac{a^4}{L}\right)^{1/3}\ln\left(\frac{\varphi_w}{\varphi_b}\right) \quad (3)$$

When dosing MPE50 at the onset of filtration (0 min), the same increase in aggregate size was not observed (Fig. 10) which suggests that the process of aggregation is favoured when a concentrated layer of biopolymers/microspheres has developed at the membrane surface. Polymeric coagulants ordinarily exhibit low diffusivities and high viscosities thus mixing is generally recommended to ensure enhanced dispersion of the polymer through the particle matrix using velocity gradients exceeding 1500 s^{-1} for up to 600 s [3]. Whilst a comparatively low shear profile was adopted in this study, it is asserted that the presence of the fluidised cake enhanced the probability for collision of destabilised particles through an applied concentration gradient which encouraged growth of large flocs. Importantly, dosing MPE50 was observed to reduce fouling whether added at the initiation of filtration or during the filtration cycle, which conforms with earlier observations [4,5]. However, residual resistance was lowest by dosing MPE50 at the onset of filtration (Fig. 8), which is ascribed to the early initiation of biopolymer aggregation which limited the development of a polarised layer of biopolymers at the membrane surface. Consequently, it is suggested that the low shear conditions initiated in MBR are not preferable to direct dosing of high concentration coagulants during filtration due to the complexity of the coagulation kinetics involved. Instead high concentration coagulant doses should be applied before or at the onset of filtration. These findings are corroborated at full scale where MPE50 dosing is recommended after chemical cleaning and before the initiation of filtration which will promote biopolymer assimilation within floc structures before permeation begins [24].

5. Conclusions

In this study, the impact of kinetically controlled floc growth on sustaining membrane permeability following reactive coagulant dosing was determined. Floc formation was indicated to comprise of two stages: (i) an initial destabilisation phase in which the charge on the protein and polysaccharide was sufficiently neutralised to encourage complexation; and (ii) entrapment of the coarse model particles (3 μm Firefli™ microspheres) in the polymeric complex during the floc growth phase. Floc growth was characterised by an expected time lag as with conventional flocculation systems and as the kinetics immediately favoured biopolymer aggregation, when coagulant was dosed during the filtration cycle, the intermediate biopolymer complexes (comprised of protein and polysaccharide) were preferentially transported toward the membrane causing fouling. In comparison, when coagulant was dosed at the onset of filtration, membrane fouling was constrained. It is asserted that by dosing at the onset of filtration: (i) early development of biopolymer aggregation is initiated which inhibits transport of the individual biopolymers to the membrane; and (ii) by dosing coagulant in the absence of a developed polarised layer, formation of biopolymer complexes local to the membrane is obviated. However, when dosing coagulant at the onset of filtration, only limited floc growth occurred which can be explained by the low applied wall shear rate and the absence of a 'polarised' region ostensibly promoting floc growth, which in turn enhances the probability for particle back-transport from the membrane. Based on results from the model particle system studied, it is proposed that reactive coagulant dosing is best undertaken in the absence of filtration and within a moderate shear environment for sufficient time to promote floc growth before filtration is initiated.

Acknowledgements

The authors would like to thank the Engineering and Physical Sciences Research Council for funding provided through the First Grant Scheme (EPSRC, EP/K010360/1) and Impact Acceleration Account. We would like to thank employees at Nalco for their support during the experimental phase of this work. The findings and conclusions contained within are those of the authors and do not necessarily reflect positions or policies of the funders, or Nalco. Enquiries for access to the data referred to in this article should be directed to: researchdata@cranfield.ac.uk.

References

[1] T. Jiang, M.D. Kennedy, C. Yoo, I. Nopens, W. van der Meer, H. Futselaar, J. C. Schippers, P.A. Vanrolleghem, Controlling submicron particle deposition in a side-stream membrane bioreactor: A theoretical hydrodynamic modelling approach incorporating energy consumption, J. Membr. Sci. 297 (2007) 141–151.
[2] H. Li, A.G. Fane, H.G.L. Coster, S. Vigneswaran, An assessment of depolarisation models of crossflow microfiltration by direct observation through the membrane, J. Membr. Sci. 172 (2000) 135–147.
[3] O.P. Sahu, P.K. Chaudhari, Review on chemical treatment of industrial wastewater, J. Appl. Sci. Environ. Manag. 17 (2013) 241–257.
[4] V. Iversen, R. Mehrez, R.Y. Horng, C.H. Chen, F. Meng, A. Drews, B. Lesjean, M. Ernst, M. Jekel, M. Kraume, Fouling mitigation through flocculants and adsorbents addition in membrane bioreactors: Comparing lab and pilot studies, J. Membr. Sci. 345 (2009) 21–30.
[5] H. Koseoglu, N.O. Yigit, V. Iversen, A. Drews, M. Kitis, B. Lesjean, M. Kraume, Effects of several different flux enhancing chemicals on filterability and fouling reduction of membrane bioreactor (MBR) mixed liquors, J. Membr. Sci. 320 (2008) 57–64.
[6] T. Wozniak, Comparison of a conventional municipal plant and an MBR plant with and without MPE, Desalin. Water Treat. 47 (2012) 341–352.
[7] F. Neemann, S. Rosenberger, B. Jefferson, E.J. McAdam, Non-covalent protein-polysaccharide interactions and their influence on membrane fouling, J. Membr. Sci. 446 (2013) 310–317.
[8] P. Côté, T. Young, S. Smoot, J. Peeters, Energy consumption of MBR for municipal wastewater treatment: current situation and potential, Proc. Water Environ. Fed. 14 (2013) 479–492.
[9] E.J. McAdam, M. Pawlett, S.J. Judd, Fate and impact of organics in an immersed membrane bioreactor applied to brine denitrification and ion exchange regeneration, Water Res. 44 (2010) 69–76.
[10] E. Reid, X. Liu, S.J. Judd, Effect of high salinity on activated sludge characteristics and membrane permeability in an immersed membrane bioreactor, Water Res. 283 (2006) 164–171.
[11] S. Delgado, R. Villarroel, E. González, Effect of the shear intensity on fouling in submerged membrane bioreactor in wastewater treatment, J. Membr. Sci. 311 (2008) 173–181.
[12] S. Jamal Khan, C. Visvanathan, V. Jegatheesan, R. Ben Aim, Influence of mechanical mixing rates on sludge characteristics and membrane fouling in MBRs, Sep. Sci. Technol. 43 (2008) 1826–1838.
[13] E.J. McAdam, S.J. Judd, E. Cartmell, B. Jefferson, Influence of substrate on fouling in anoxic immersed membrane bioreactors, J. Membr. Sci. 41 (2007) 3859–3867.
[14] B.-K. Hwang, W.-N. Lee, P.-K. Park, C.-H. Lee, I.-S. Chang, Effect of membrane fouling reducer on cake structure and membrane permeability in membrane bioreactor, J. Membr. Sci. 288 (2007) 149–156.
[15] A. Drews, membrane fouling in membrane bioreactors – Characterisation, contradictions, cause and cures, J. Membr. Sci. 363 (2010) 1–28.
[16] K. Yamamoto, M. Hiasa, T. Mahmood, T. Matsuo, Direct solid-liquid separation using hollow fibre membrane in an activated sludge aeration tank, Water Sci. Technol. 21 (1989) 43–54.

[17] P. Cote, H. Buisson, C. Pound, G. Arakaki, Immersed membrane activated sludge for the reuse of municipal wastewater, Desalination 113 (1997) 189–196.
[18] E.J. McAdam, E. Cartmell, S.J. Judd, Comparison of dead-end and continuous filtration conditions in a denitrification membrane bioreactor, J. Membr. Sci. 369 (2011) 167–173.
[19] O. Autin, E.J. McAdam, Method and apparatus for monitoring particles in a liquid, GB Patent Application No. 1516481.7 (2015).
[20] S.-H. Yoon, J.H. Collins, D. Musale, S. Sundararajan, S.-P. tsai, G.A. Hallsby, J. F. Kong, J. Koppes, P. Cachia, Effects of flux enhancing polymer on the characteristics of sludge in membrane bioreactor process, Water Sci. Technol. 51 (2005) 151–157.
[21] I.S. Chang, P. Le Clech, B. Jefferson, S. Judd, membrane fouling in membrane bioreactors for wastewater treatment, J. Environ. Eng. (2002) 1018–1029.
[22] S. Rosenberger, C. Laabs, B. Lesjean, R. Gnirss, G. Amy, M. Jekel, J.-C. Schrotter, Impact of colloidal and soluble organic material on membrane performance in membrane bioreactors for municipal wastewater treatment, Water Res. 40 (2006) 710–720.
[23] A. Drews, J. Mante, V. Iversen, M. Vocks, B. Lesjean, M. Kraume, Impact of ambient conditions on SMP elimination and rejection in MBRs, Water Res. 41 (2007) 3850–3858.
[24] T. Wozniak, MBR design and operation using MPE-technology (Membrane Performance Enhancer), Desalination 250 (2010) 723–728.
[25] S. Nataraj, R. Schomacker, M. Kraume, I.M. Mishra, A. Drews, Analyses of polysaccharide fouling mechanisms during crossflow membrane filtration, J. Membr. Sci. 308 (2008) 152–161.
[26] Y. Marselina, Lifia, P. Le-Clech, R.M. Stuetz, V. Chen, Characterisation of membrane fouling deposition and removal by direct observation technique, J. Membr. Sci. 341 (2009) 163–171.
[27] B. Frolund, R. Palmgren, K. Keiding, P.H. Nielsen, Extraction of extracellular polymers from activated sludge using a cation exchange resin, Water Res. 30 (1996) 1749–1758.
[28] M. Dubois, K.A. Gilles, J.K. Hamiltin, P.A. Rebers, F. Smith, Colorimetric method for determination of sugars and related substances, Anal. Chem. 28 (1956) 350–356.
[29] E.J. McAdam, S.J. Judd, Immersed membrane bioreactors for nitrate removal from drinking water: Cost and feasibility, Desalination 231 (2008) 52–60.
[30] B.-M. Wilén, B. Jin, P. Lant, The influence of key chemical constituents in activated sludge on surface and flocculating properties, Water Res. 37 (2003) 2127–2139.
[31] O. Ojajuni, S. Holder, G. Cavalli, J. Lee, D.P. Saroj, Rejection of caffeine and carbamazepine by surface-coated PVDF hollow-fiber membrane system, Ind. Eng. Chem. Res. 55 (2016) 2417–2425.

Investigating the significance of coagulation kinetics on maintaining membrane permeability in an MBR following reactive coagulant dosing

Autin, Olivier

2016-06-11

Autin O, Hai F, Judd S, McAdam EJ, (2016) Investigating the significance of coagulation kinetics on maintaining membrane permeability in an MBR following reactive coagulant dosing. Journal of Membrane Science, Volume 516, October 2016, pp. 64-73

http://dx.doi.org/10.1016/j.memsci.2016.06.008